

MOUSE LV 3D MOTION AND STRAIN ANALYSIS USING TAGGED MRI

Yang Yu*, Shaoting Zhang*, Zhennan Yan*, Song Chen[†], Rong Zhou[†], Dimitris Metaxas*

* Department of Computer Science, Rutgers University, Piscataway, NJ, 08854 USA

[†] Department of Radiology, University of Pennsylvania, Philadelphia, PA, 19104 USA

ABSTRACT

This paper presents a framework to reconstruct mouse left ventricular motion based on tagged MRI using nonlinear Laplacian deformable models, which perform better in terms of accuracy and efficiency. Based on the deformation results, we analyze the LV 3D motion and strain of the myocardial wall to depict the contractile function of the heart. In our framework, the 2D tagging lines are extracted using active contour models. The 3D control points are then generated from the intersections of the tagging lines, and a 3D meshless model is built based on the sparse 2D contours. Finally, the initial model is driven to deform by the control points using 3D meshless deformable model with nonlinear Laplacian kernel. This method is validated using the in vivo MRI tagging data from the mouse heart. The results show that the proposed method effectively quantifies the myocardial strain distribution of the LV model in 3D, which has the potential to increase accuracy in detecting various kinds of heart diseases.

Index Terms— Tagged MRI, strain analysis, mouse cardiac, deformable model

1. INTRODUCTION

Over the past two decades, experiments utilizing transgenic and knockout mice have significantly advanced the research on cardiovascular diseases, and these models have become an indispensable tool to study the cardiovascular diseases in humans [6, 16]. The majority of such studies have employed ex vivo methods (e.g. immunostaining) for assessing the results of gene manipulation, and, for the heart function, catheter-based measurements of left-ventricular (LV) pressure in isolated Langendorff-perfused hearts are obtained. For the study of ventricular function in particular, noninvasive imaging offers a powerful non-invasively tool for making measurements that directly reflect its complex in vivo physiology.

Tagged magnetic resonance imaging (MRI) has been widely used to analyze the cardiac wall motion [1]. It is used to diagnose human heart diseases as well as experimental heart disease models in mice. Since the development of tagged MRI, many methods have been developed to analyze the human heart [10], but not all of them can be applied directly to the mouse cardiac data due to its low quality.

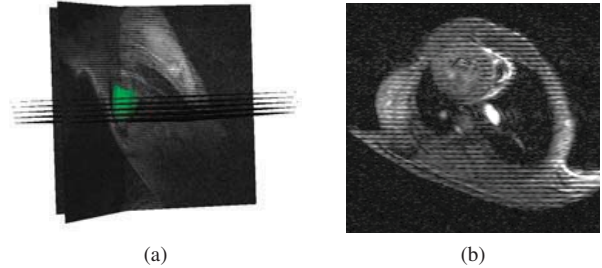


Fig. 1: (a) The setting of MR images with fitted LV model rendered in green: five SA images parallel placed with equal displacements, and four LA images taken with 45° in between. (b) Tagged SA image. The image resolution is low, and the tagging lines are blurred due to fast heart beating.

Compared with the human heart, the data acquisition process for the mouse heart is more challenging to achieve adequate spatial and temporal resolution. The mouse heart is about 1000th the size of a human heart and beats at 400-600 beats per minute (bpm), which is much faster than a human heart (60-80 bpm). Currently available MRI instruments for mouse imaging operate at a higher magnetic field strength (4.7T or above) than clinical MRI scanners but is still unable to provide temporal and spatial resolution in proportion with the mouse heart rate and size. Consequently, a compromise is obtained between tagging spatial and temporal resolution. As shown in Fig.1a, there are only five short-axis (SA) and four long-axis (LA) MR images. The SA images are too sparse, so that there is no continuity between adjacent ones. The registration-based methods [2] require more slices of SA images in order to register each pixel to the following frame with proper displacement on LA direction. The large gaps between SA images make the 3D registration infeasible. In addition, as shown in Fig.1b, the tagging lines on each MR images show high intensity with very small spaces in between. This increases error rate during 2D tagging tracking process due to mis-tracking adjacent ones, especially in vague images. In this paper, we propose nonlinear deformable models to reconstruct 3D motions, which experimentally prove high accuracy in processing sparse 2D MRI data.

The 2D characterization of the murine cardiac mechanical function in normal, infarcted, or genetically engineered mice

or rat model subjected to stem cell intervention have been reported in [4, 7, 16]. Recently studies drew more attention on the analysis of complete 3D LV strain. Zhong et al. [15] presented the 3D myocardial deformation based on the movement of SA tagging intersection points. The motion of these points are easy to be acquired, but the estimation may contain bias since they cluster at only a few SA slices. Chuang et al. [3] reconstructed the LV motion by linear interpolating the displacement of the intersection points in short and long axis separately. The result is only a linear approximation of the complex myocardial motion. It is hard to maintain accuracy when the MR images are sparse. Though Young et al. [13] proposed more sophisticated methods to smooth the interpolation, the displacements of the material points were still intrinsically linearly interpolated, and the results did not show remarkable improvement under sparse MR images.

In this paper, we propose a new nonlinear meshless deformation framework, namely *meshless model* as the *representation* and *nonlinear Laplacian method* as the *deformation kernel*, for 3D LV motion analysis problem. Meshless deformable models have been demonstrated to be robust by being widely investigated in mechanical simulation [11]. Experimental results prove their efficiency in saving construction and maintenance cost, compared to mesh-based models. Among the various kernels for deformation in meshless models, Laplacian kernels are very efficient in computation speed [11]. However, as a linear approximation of physics-based models, they cannot fully depict the motion of points on the cardiac model when nonlinear deformation, like rotation and twisting, happens. Kernels derived from continuum mechanics [12] have relatively high degrees of freedom, but they are sensitive to parameters and have high computational complexity. In our paper, the proposed nonlinear Laplacian kernel inherits the computational advantage of the Laplacian method, while reconstructing the complex LV motion with high accuracy due to its nonlinear nature. We validate this algorithm based on simulation of the mouse LV deformation.

2. METHODOLOGY

System Framework: A complete system is built to reconstruct the deformable model from the sparse images. It consists of four major components: 1) tagging line tracking, 2) control point tracking, 3) meshless model construction, 4) meshless deformation. Active contour models are implemented to robustly track the tags for low quality tagged MR images, and the 2D LV contours are automatically delineated under deformable models. Then the initial 3D meshless model of the ED LV is built using the modified coherent point drift [8] based on the sparse contour. Traditional tracking methods can handle sparse landmarks effectively in cine MR images [17]. In our application, the intersections of the tags provide more dense control points with detail movements. Using our proposed nonlinear deformable model, the initial

Algorithm 1 Nonlinear Laplacian deformation

Input: the positions of the initial points \mathbf{p} , and the control points \mathbf{c}

Output: the positions \mathbf{p}' after deformation

precalculate the weight ω_{ij} , and the initial guess \mathbf{p}'_0

repeat

for each i , calculate local rotation \mathbf{R}_i from \mathbf{S}_i in (3)

solve linear system (4) to get the new position \mathbf{p}'

for all $k \in \mathcal{F}$, set \mathbf{p}'_k as \mathbf{c}_k

until \mathbf{p}' converges.

model is driven by the control points to demonstrate the LV movement along a cardiac cycle. The motion strains are calculated locally based on the movement of the point cloud.

Meshless Models with Nonlinear Laplacian Kernel:

Different from the traditional simulation methods, the meshless model abandons the grid or mesh structures, using only the particles to represent the model [11]. It is widely used in problems with large deformations and nonlinear material behavior. Meanwhile, the complex and sensitive mesh generation process is eliminated. The material point is considered as the center of the phixel which is a sphere with radial decreasing mass distribution. Given a dense phixel representation, any point on the model is expressed as the weighted average of all the phixels whose ranges cover this position. The mechanical properties, like mass and density, are all defined in this manner.

Many deformable models have been proposed under the meshless framework. Usually, some kinds of internal forces are used to express the interactions among the phixels based on the special material properties. The myocardial wall is considered as nearly incompressible, which is experimentally proved that the volume change is no more than 4% [10]. So we propose a constraint that all the material points keep the distances to the nearby points. Similar constraint has been used for surface mesh deformation in [9] to preserve the surface detail, while we use it to maintain the shape on 3D volume model. In the neighborhood of any vertex i , the distance-preserve deformation is approximated as rotation:

$$\mathbf{p}'_i - \mathbf{p}'_j = \mathbf{R}_i(\mathbf{p}_i - \mathbf{p}_j) + \varepsilon, \forall j \in \mathcal{N}(i). \quad (1)$$

where \mathbf{p}_i and \mathbf{p}'_i are the positions of the vertex i at the initial and the following frame, \mathbf{R}_i is the rotation matrix at the vertex i , and $\mathcal{N}(i)$ is the neighborhood of the vertex i . The actual movement of the point set may not be presented as rotation. However, a deformation under the proposed constraint is achieved by minimizing the error ε . Given the control point positions after deformation, the positions of all the points will be calculated by minimizing the following energy function:

$$\min_{\mathbf{p}', \mathbf{R}} \sum_{i=1}^n \sum_{j \in \mathcal{N}(i)} \omega_{ij} \|(\mathbf{p}'_i - \mathbf{p}'_j) - \mathbf{R}_i(\mathbf{p}_i - \mathbf{p}_j)\|^2 \quad (2)$$

s.t. $\mathbf{p}'_k = \mathbf{c}_k, k \in \mathcal{F}$

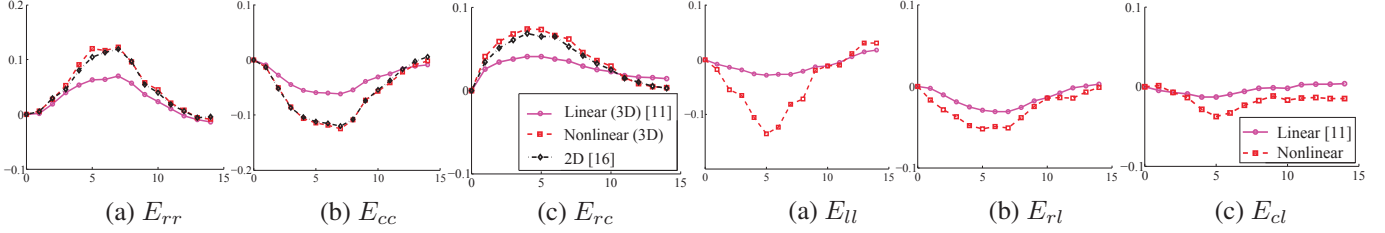


Fig. 2: Comparing the 3D strains from the linear [11] and our nonlinear models with the 2D strains [16] in a cardiac cycle, including radial (E_{rr}), circumferential (E_{cc}) and radial-circumferential (E_{rc}) strains.

where ω_{ij} is a fixed weight, which decreases as the distance between the two points increasing in the initial frame. \mathcal{F} is the set of indices of the control points with position c_k . The energy term for each phyxel relates only to the Laplacian coordinate change under rotation. The Laplacian coordinate was also used in [11], where the scaling and rotation matrix was used for transformation. However, only the linear component was estimated to approximate the rotation. This limits the method for small deformation. The nonlinear model usually achieves better accuracy with more complex computation. In our work, the nonlinear system can be efficiently solved by iteratively optimizing the position and the rotation matrices.

Given the position \mathbf{p}'_i after the deformation, the optimal rotation \mathbf{R}_i can be solved separately for each vertex i . We define the weighted covariance matrix between the initial and deformed positions of vertex i based on its neighbor vertices j as:

$$\mathbf{S}_i = \sum_{j \in \mathcal{N}(i)} \omega_{ij} (\mathbf{p}_i - \mathbf{p}_j) (\mathbf{p}'_i - \mathbf{p}'_j)^T \quad (3)$$

Supposing the singular value decomposition of \mathbf{S}_i is $\mathbf{U}_i \mathbf{\Sigma}_i \mathbf{V}_i^T$, \mathbf{R}_i can be derived as $\mathbf{R}_i = \mathbf{V}_i \mathbf{U}_i^T$.

Then with the updated optimal rotation matrix \mathbf{R} , the minimum of (2) can be achieved by the following linear functions for all the vertex i :

$$\sum_{j \in \mathcal{N}(i)} \omega_{ij} (\mathbf{p}'_i - \mathbf{p}'_j) = \sum_{j \in \mathcal{N}(i)} \frac{\omega_{ij}}{2} (\mathbf{R}_i + \mathbf{R}_j) (\mathbf{p}_i - \mathbf{p}_j) \quad (4)$$

All the linear functions can build a sparse linear system, with the Laplace operator applied to \mathbf{p}' . The control points will always keep their given positions, while the positions of the other points will be updated based on the solution of the linear system. Based on the above method, \mathbf{p}' and \mathbf{R} are solved iteratively. With an initial guess of the positions \mathbf{p}'_0 , we solve the non-linear problem iteratively by algorithm 1.

Strain Analysis: 3D strains are estimated by computing the spatial gradients of the displacement field. The resulting strains in Cartesian space are converted to LV-oriented coordinates. This permits us to access the radial, longitudinal, and circumferential strains of the LV.

Fig. 3: Comparing the 3D strains from our nonlinear models with that from the linear ones [11] in a cardiac cycle, including longitudinal (E_{ll}), radial-longitudinal (E_{rl}) and circumferential-longitudinal (E_{cl}) strains. Note that 2D strains cannot cover these directions.

3. EXPERIMENTS

Experimental settings: Nine mice were examined on a 4.7T Varian INOVA system. Both of the SPAMM tagged images and cine image were acquired within the whole cardiac cycle. Two sets of tagged SA images were acquired with tagging planes perpendicular to each other in each slice. Then, four slices in LA views were chosen radially spaced every 45° . The tagging plane on the LA slices were parallel to the SA. This made the three tagging planes all perpendicular to each other, which is the minimum requirement for the reconstruction of the 3D motion for the heart. The non-tagged images were also acquired for both the LA and SA slices mentioned above at the same time step as the tagged ones, which were used for the segmentation of the heart boundary.

In [16], the 2D mouse LV strains were calculated based on the movement of intersection points on the SA slices, which is proved to be consistent with previous researches. Here, taking their results as standard, we compare the global strains calculated from our nonlinear deformation method with that from the 3D deformation method based on linear Laplacian kernel in [11].

Fig. 2 shows comparison results between our models and models in [11] in terms of radial, circumferential normal strains and radial-circumferential shear strains. The resulting strains of our nonlinear models are similar to the 2D ones, with average difference 5%, while the differences from the linear models are around 40%. Our nonlinear Laplacian kernel shows better accuracy than the linear one [11] in above comparison. It further proves that the nonlinear deformable models have better performance in heart motion simulation.

The strains related to the longitudinal direction cannot be estimated based on 2D intersection point movement. The 3D methods naturally present them. The strains outside the SA slices are shown in Fig. 3. Similar to the other strains, the nonlinear kernel gives larger strains. The magnitude of the strains from the linear kernel is less than 50% of that from nonlinear one. Similar to the SA results, the linear kernel

tends to underestimate the magnitude of the strains.

All the methods are implemented using C++ on an Intel i7 2.80GHz computer with 8GB RAM. The computing time for the nonlinear deformation on 15 frames (a cardiac cycle) is around 40 seconds, which is comparable to the linear one. The similar preprocesses which construct the Laplacian matrices for both methods take up the majority of the time. In addition, the iterative method to solve nonlinear Laplacian kernel often converges in less than ten steps. Therefore, our nonlinear deformable models improve the simulation accuracy without sacrificing the computational efficiency.

4. CONCLUSION

In this work, we present a comprehensive framework to analyze the mouse LV motion using the tagged MRI. The whole process is optimized to track the movement of the mouse heart robustly during the cardiac cycle. The 3D meshless LV model is built and deformed based on the nonlinear Laplacian kernel. The experiments show that it can simulate the LV motion better than the linear one in terms of accuracy. Based on the deformable model, strains are quantified at every local point, which enables us to analyze properties of the ventricular wall locally and globally. The framework may also be applied to the human heart MR images to overcome the insufficiency of the SA slices and the low image quality.

Our nonlinear deformable models are designed based on the volume preserving property of the myocardium. In the future, we will investigate the connection between our models and the physical-based ones. This will inspire us to design new deformable models with more sophisticated physical properties while maintaining the computational efficiency. Furthermore, the 2D tagging line tracking results on the tagged MR images may contain sparse outliers. They often seriously affect the whole model. Therefore, we expect to utilize compressed sensing technique [14, 5] to reduce their influence and increase the robustness of deformable models.

We thank Dr. Xin Yu for providing the mouse cardiac MRI dataset and Dr. Wei Li for manually labeling the data.

5. REFERENCES

- [1] E. Castillo, J. A. C. Lima, and D. A. Bluemke. Regional myocardial function: Advances in MR imaging and analysis. *Radiographics*, 23:127–140, 2003.
- [2] R. Chandrashekhara, R. Mohiaddin, and D. Rueckert. Analysis of 3-D myocardial motion in tagged MR images using nonrigid image registration. *TMI*, 23(10):1245–1250, Oct. 2004.
- [3] J. S. Chuang, A. Zemljic-Harpf, R. S. Ross, L. R. Frank, A. D. McCulloch, and J. H. Omens. Determination of three-dimensional ventricular strain distributions in gene-targeted mice using tagged MRI. *MRM*, 64(5):1281–1288, 2010.
- [4] F. H. Epstein, Z. Yang, W. D. Gilson, S. S. Berr, C. M. Kramer, and B. A. French. MR tagging early after myocardial infarction in mice demonstrates contractile dysfunction in adjacent and remote regions. *MRM*, 48(2):399–403, 2002.
- [5] J. Huang, S. Zhang, and D. Metaxas. Efficient mr image reconstruction for compressed mr imaging. *Medical Image Analysis*, 15(5):670–679, 2011.
- [6] R. L. Janiczek, B. R. Blackman, R. J. Roy, C. H. Meyer, S. T. Acton, and F. H. Epstein. Three-dimensional phase contrast angiography of the mouse aortic arch using spiral MRI. *MRM*, 66(5):1382–1390, 2011.
- [7] W. Liu, M. W. Ashford, J. Chen, M. P. Watkins, T. A. Williams, S. A. Wickline, and X. Yu. MR tagging demonstrates quantitative differences in regional ventricular wall motion in mice, rats, and men. *Am J Physiol Heart Circ Physiol*, 291(5):2515–2521, 2006.
- [8] A. Myronenko and X. Song. Point set registration: Coherent point drift. *TPAMI*, 32(12):2262–2275, 2010.
- [9] O. Sorkine and M. Alexa. As-rigid-as-possible surface modeling. In *SGP*, pages 109–116, 2007.
- [10] H. Wang and A. A. Amini. Cardiac motion and deformation recovery from MRI: A review. *TMI*, 31(2), 2012.
- [11] X. Wang, T. Chen, S. Zhang, D. Metaxas, and L. Axel. LV motion and strain computation from tMRI based on meshless deformable models. In *MICCAI*, volume 5241, pages 636–644. 2008.
- [12] K. Wong, L. Wang, H. Zhang, H. Liu, and P. Shi. Physiological fusion of functional and structural images for cardiac deformation recovery. *TMI*, 30(4), 2011.
- [13] A. A. Young, B. A. French, Z. Yang, B. R. Cowan, W. D. Gilson, S. S. Berr, C. M. Kramer, and F. H. Epstein. Reperfused myocardial infarction in mice: 3D mapping of late gadolinium enhancement and strain. *JCMR*, 8(5):685–692, 2006.
- [14] S. Zhang, Y. Zhan, M. Dewan, J. Huang, D. N. Metaxas, and X. S. Zhou. Towards robust and effective shape modeling: Sparse shape composition. *Medical Image Analysis*, 16(1):265–277, 2012.
- [15] J. Zhong, W. Liu, and X. Yu. Characterization of three-dimensional myocardial deformation in the mouse heart: An MR tagging study. *JMRI*, 27(6), 2008.
- [16] R. Zhou, S. Pickup, J. D. Glickson, C. H. Scott, and V. A. Ferrari. Assessment of global and regional myocardial function in the mouse using cine and tagged MRI. *MRM*, 49(4):760–764, 2003.
- [17] Y. Zhou, E. Yeniaras, P. Tsiamyrtzis, N. Tsekos, and I. Pavlidis. Collaborative tracking for MRI-guided robotic intervention on the beating heart. In *MICCAI*, volume 6363, pages 351–358. 2010.